

Biosorption characteristic of *Alcaligenes* sp. BAPb.1 for removal of lead(II) from aqueous solution

Yu Jin¹ · Sumei Yu¹ · Chunying Teng¹ · Tao Song¹ · Liying Dong¹ · Jinsong Liang¹ · Xin Bai¹ · Xiuhong Xu¹ · Juanjuan Qu¹

Received: 30 November 2016 / Accepted: 6 April 2017 / Published online: 31 May 2017
© Springer-Verlag Berlin Heidelberg 2017

Abstract In this study, strain BAPb.1 was isolated from lead mining area and used as an adsorbent to remove lead(II) ions from aqueous solution. The physicochemical characteristics, heavy metal resistance and antibiotic sensitivity of strain BAPb.1 were investigated. Biosorption capacity was evaluated by batch biosorption experiments, and isothermal characteristics were discussed. Atomic force microscopy (AFM), scanning electron microscopy (SEM), energy dispersive X-ray spectroscopy (EDX) and Fourier transform infrared spectrometry (FTIR) were conducted to explore the mechanism for lead(II) adsorption. Based on morphological and physiological characteristics as well as the phylogenetic analysis of 16S rDNA sequences, strain BAPb.1 was identified as a member of the genus *Alcaligenes*. It exhibited high resistances to multiple heavy metals such as lead(II), copper(II), zinc(II), nickel(II) and chromium(VI), and to antibiotics such as kanamycin, ampicillin, streptomycin, chloramphenicol, and tetracycline. The optimum conditions for maximum biosorption rate of 85.2% and maximum capacity of 56.8 mg g⁻¹ were found at pH of 5, adsorbent dosage of 1.5 g L⁻¹ (dry weight), initial lead(II) concentration of 100 mg L⁻¹, and contact time of 30 min at 30 °C. Biosorption isotherms were well fitted with Langmuir isotherm model. Mechanism analysis reveals that the lead(II) ions may exchange with sodium and potassium ions, and the hydroxyl, carbonyl and phosphate groups on the cell surface can chelate the lead(II) ions, therefore, surface adsorption play significant role in the biosorption process.

Keywords Heavy metals · Biosorption · Lead(II) · Characteristics · *Alcaligenes* sp.

Introduction

The water discharged or leached from the mining areas is often polluted by heavy metals, which even at trace level is harmful to the health of human beings and eco-system (Gupta et al. 1998; Khani et al. 2010; He and Chen 2014; Latha et al. 2015). Lead (Pb) is a malleable and heavy post-transition metal generally applied in building construction, e-manufacturing, mining, lead-acid battery and so on (Gupta et al. 2011; Saleh et al. 2013). China is the main production and consumption country of Pb with annual output near to 135 million tons and consumption rate of 80 million tons. Moreover, backward technology, outdated equipment and unawareness of environment protection for Chinese enterprise aggravate the Pb contamination in ecological environment. Pb generally enters into human body through inhalation, ingestion, dermal contact, or transfer via the placenta. Acute and chronic exposure to Pb may cause anemia, liver and kidney disease, as well as central and peripheral nervous system damage (Özcan et al. 2009; Zhu et al. 2014). Young children are most vulnerable to Pb contamination, resulting in stunted growth and elevated blood Pb levels (BLLs) (Puyen et al. 2012).

In China, the threshold limit of Pb-containing liquid from sewage and industrial effluents has been set to 1.0 mg L⁻¹ (Environmental Quality Standard for Surface Water of China, GB8978-1996), but wastewater without efficient handling is hard to achieve the discharge standard. Many techniques such as ionic exchange, membrane separation and activated carbon adsorption are taken to

✉ Juanjuan Qu
juanjuan4050234@163.com

¹ College of Resource and Environment, Northeast Agricultural University, Harbin 150030, China

remove lead ions from aqueous waste to ensure environmental safety, but these measures commonly require special equipment and rigorous experimental condition (Congeevaram et al. 2007). Biosorption process utilizes various natural materials possessing metal sequestering properties, which decrease the concentration of heavy metal ions in solution from ppm to ppb level. Furthermore, the biosorbents are readily available biomass from nature and have more distinct advantages, such as low cost and high adaptability to small-scale industries (Ucuna et al. 2009; Gupta and Nayak 2012). Three commercial biologicals including *Chlorella vulgaris*, *Bacillus* sp. and yeast have been exploited for heavy metal treatment by B.V.SORBEX Inc. Visa Tech Ltd. and US Bureau of Mines, respectively (Gabr et al. 2008). Currently more and more bacterial biomaterials have been applied in heavy metal removal (Huang et al. 2013). The functional groups (amino, hydroxyl, carboxyl and sulfate) of polysaccharides, proteins and lipids on their cell walls can act as binding sites to attract and combine metals (Ng et al. 2009).

In the light of above facts, the present study aims to screen out a bacterial isolate from the lead mining area which can sustain high concentration of lead(II), and study its biosorption characteristics under various conditions, and reveal its possible mechanism by Atomic force microscopy (AFM), energy dispersive X-ray spectroscopy (EDX), Fourier transform infrared spectrometry (FTIR) techniques. These studies confirm the feasibility of the bacterium for the removal of toxic heavy metal lead(II) from wastewaters.

Materials and methods

Isolation and identification of lead resistant bacterium

To obtain the lead resistant bacterium, 100 g soil samples were collected from ten randomly selected sampling points (each point 10 g) in a Pb mine (Pb concentration was 2.0–3.5 g kg⁻¹) in Heilongjiang Province, China. One gram of soil was homogenized with 100 mL of sterile distilled water, and this soil suspension was serially diluted until a dilution of 10⁻⁵. Luria–Bertani (LB) agar medium contained serial concentrations (200–1000 mg L⁻¹) of lead(II) [as Pb(NO₃)₂] were applied to select lead resistant bacterium. 0.2 mL of soil suspension (10⁻⁵) was plated on these LB agar plates using standard plate dilution method (Sheng et al. 2008). Agar plates were incubated at 30 °C for 3–4 days. Single colonies were picked and streaked onto a new LB agar plate for three times to obtain the pure isolates. The preliminary morphological, biochemical, and physiological characterizations of the pure isolates have

been carried out according to the methods of Dong and Cai (2001), the 16S rDNA sequence analysis was referred to the method of Batta et al. (2013).

Heavy metal resistance and antibiotic sensitivity

The bacterial isolate was studied for its resistance to heavy metals and sensitivity to antibiotics. The exponential phase culture of bacterial isolate was inoculated aseptically on LB agar medium supplemented with heavy metals such as lead(II), copper(II), zinc(II), nickel(II), and chromium(VI). The metal salts used were Pb(NO₃)₂, CuSO₄, ZnCl₂, NiCl₂, and K₂Cr₂O₇ (Analytical reagent, Kermel, Tianjin, China) at concentrations ranging from 100 to 1200 mg L⁻¹. The growth was observed after 24-h incubation up to 48 h at 30 °C. Susceptibility to different antibiotics (kanamycin, ampicillin, streptomycin, chloramphenicol, and tetracycline) at a concentration ranging from 10 to 50 µg mL⁻¹ was determined by agar disk diffusion method. The bacterial isolate was classified as resistant or susceptible by examining the zone of inhibition on the lawn of bacterial culture after incubated for 24 h at 30 °C (Tripathi et al. 2011).

Preparation of biosorbent and lead(II) solution

The lead resistant strain was inoculated into sterile LB liquid medium and cultivated in a thermostatic shaker at 30 °C. The live cells were harvested at late exponential phase by centrifugation at 8000 rpm for 10 min, then washed with phosphate buffered saline (PBS) and deionized water. The cells were frozen dried and ground into powder using mortar and pestle. This dead and powdered biomass was stored in a desiccator for the biosorption experiments.

The standard stock solution of lead(II) of 5 g L⁻¹ was prepared by dissolving a certain amount of Pb(NO₃)₂ in deionized water. The stock solution was further diluted to the required concentrations before use.

Batch biosorption experiments

Batch biosorption experiments were carried out as functions of pH, initial lead ion concentration, biosorbent dosage, and contact time in 250 mL Erlenmeyer flasks in a thermostatic shaker. The flasks were agitated with a rotational speed of 160 rpm at 30 °C, and the pH value was adjusted with 0.5 M HCl or 0.5 M NaOH solution. The influences of initial lead(II) concentration (10–150 mg L⁻¹), pH (3–7), biosorbent dosage (0.5–4.0 g L⁻¹), temperature (22–40 °C) and contact time (5–50 min) were evaluated.

After the solution was centrifuged and filtered, lead(II) concentration of the supernatant was determined by atomic absorption spectrophotometer (AAS) (AA-6800, Shimadzu-GL, Japan). The experiments were conducted in triplicate and the mean values were calculated. Finally, the Q (biosorption rate, %) and the q (adsorption capacity, mg g^{-1}) were calculated using Eqs. (1) and (2), respectively,

$$Q = \frac{(C_0 - C)}{C_0} \times 100\% \quad (1)$$

$$q = \frac{C_0 - C}{M} \times V \quad (2)$$

where, C_0 and C are the initial and final concentrations of lead(II) (mg L^{-1}). The V and M are the volume of solution (mL) and the weight of adsorbent (g), respectively.

The Langmuir and Freundlich isotherm models were carried out by conducting biosorption experiments with different initial lead(II) concentrations (Freundlich 1906; Langmuir 1918). The experimental data conformed to the linear form of Langmuir and Freundlich model expressed as the following Eqs. (3) or (4), respectively,

$$\frac{1}{q_e} = \frac{1}{q_m} + \frac{1}{K_L \times q_m} \times \frac{1}{C_e} \quad (3)$$

$$\ln q_e = \ln K_F + \frac{1}{n} \times \ln C_e \quad (4)$$

where, q_m and K_L are Langmuir constants related to biosorption capacity (mg g^{-1}) and the energy of adsorption (L mg^{-1}); C_e is equilibrium concentration of the metal (mg L^{-1}) and q_e is the amount of the metals (mg) adsorbed by BAPb.1; (g) K_F and $1/n$ are Freundlich constants which are related to the maximum adsorption capacity and adsorption intensity, respectively.

Biosorption mechanism

AFM analysis

To obtain complementary information, whole cells were examined by Nanoscope III α atomic force microscope (AFM) (Digital Instruments, Santa Barbara, CA, USA). Both Pb-loaded and Pb-unloaded cells were collected by centrifugation, lightly rinsed in a sterile PBS solution and sterile deionized water, and then the specimens were transferred to glass slides and examined in air by AFM.

SEM-EDX analysis

The surface morphology of the strain BAPb.1 before and after lead(II) biosorption was characterized using a scanning electron microscope (SEM) (QuANTA200 model,

FEI, USA). The elements were analyzed by an energy dispersive X-ray analysis system (EDX) (QuANTA200 model, FEI, USA). Prior to analysis, the samples were coated with a thin layer of gold under an argon atmosphere to improve electron conductivity and image quality.

FTIR analysis

Spectral analysis of the strain BAPb.1 (before and after biosorption) was done using an FTIR spectrometer (Alpha, Bruker, Germany) in the region of $4000\text{--}400\text{ cm}^{-1}$. The biosorbents were pressed into spectroscopic-quality KBr pellets with a sample/KBr ratio of 1/150 and scanned for functional groups on cell surface.

Results and discussion

Characteristics of the strain

The culture grew well in 1000 mg L^{-1} lead(II) LB agar plate was isolated and designated as BAPb.1. The strain BAPb.1 is an aerobic, short rod shaped, flagella peritrichous (Fig. 1), and gram-negative bacteria. Colonies on LB solid plates were milky white to yellow in color, spherical, shiny, smooth, raised, and mucoid. The strain BAPb.1 grew evenly in LB liquid medium, forming biofilm on the top and sticky precipitate at the bottom. When grew on beef extract peptone agar medium and carbohydrates agar medium, most of the colonies appeared small irregular

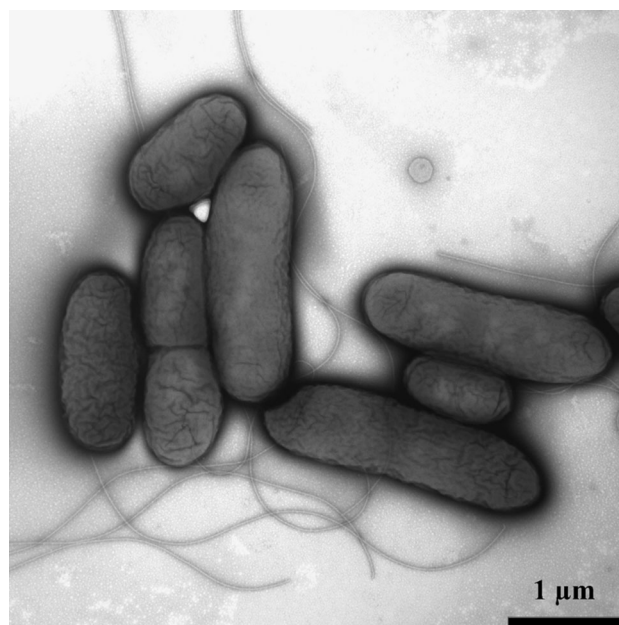


Fig. 1 The transmission electron microscope (TEM) graph of BAPb.1

margin, and produced ammonia, raising the pH value. Physicochemical characteristics of the strain were showed as follows: (+) citrate, (+) indole test, (+) methyl red, (+) gelatin liquefaction, (+) Vopes–Prokauer (V–P), and (–) D-mannose (Fig. 2).

The 16S rRNA gene of the strain BAPb.1 was cloned with the following PCR primer pairs: 16 F (5'-AGAGTTTGATCCTGGCTCAG-3') and 16R (5'-GGTTACCTTGTTACGACTT-3'). The reaction conditions were 94 °C for 5 min, 94 °C for 1 min, 58 °C for 45 s, 72 °C for 1 min, 30 cycles, and 72 °C for 10 min. The PCR products were sequenced by the BGI Biotechnology Company (Beijing) and the obtained sequence was deposited in GenBank under accession number of KC337149. Based on multiple sequence alignment done by ClustalW and phylogenetic analysis by MEGA 5 (Fig. 3), strain BAPb.1 was found to have a close relationship with *Alcaligenes* sp. thus, it was identified as a species belonging to the genus *Alcaligenes*. *Alcaligenes* species were commonly found at polluted sites with chemical or metal resistance such as strain *Achromobacter* sp. AO22(EU696789) with a lead and copper tolerance (Ng et al. 2009) and BEN-4 (AY027504) with an arsenite-oxidizing capacity (Liu et al. 2012).

Heavy metal resistance and antibiotic sensitivity

Alcaligenes sp. BAPb.1 could grow on the plates containing 1000 mg L⁻¹ lead(II), 600 mg L⁻¹ copper(II), 600 mg L⁻¹ zinc(II), 400 mg L⁻¹ nickel(II) and 400 mg L⁻¹ chromium(VI), which suggested its broad resistance to heavy metals. On the other hand, the strain BAPb.1 also could flourish on the plates containing 25 µg mL⁻¹ kanamycin, 20 µg mL⁻¹ ampicillin, 30 µg mL⁻¹ streptomycin, 20 µg mL⁻¹ chloramphenicol and 20 µg mL⁻¹ tetracycline. It has been reported that heavy metal resistance is likely to link with antibiotic resistance (Ren et al. 2015). The results of resistant experiments indicate that *Alcaligenes* sp. BAPb.1 is more adaptable to environmental contamination, and this characteristic has also been found in *Enterobacter*, *Aeromonas*, *Moraxella*, *Pseudomonas*, and *Bacillus* (Souza et al. 2006; Akinbowale et al. 2007).

Batch biosorption experiments

Effect of initial lead(II) concentration

Initial metal concentration can affect the adsorption efficiency greatly (Saleh et al. 2013). In this study, experiments were conducted firstly to investigate the effect of lead ion amount on biosorption. The initial lead(II) concentration was adjusted to the range of 10–150 mg L⁻¹ under pH 5.5, contact temperature of 30 °C, biosorbent dosage of 2 g L⁻¹ and rotational speed of 160 rpm for 30 min. Figure 4a shows that the biosorption rate decreased from 97.8 to 65.8% with the initial lead(II) concentration increased from 10 to 150 mg L⁻¹. On the other hand, the biosorption capacity rapidly increased from 4.9 to 44.1 mg g⁻¹ with the initial lead(II) concentration increased from 10 to 100 mg L⁻¹ and then kept stable when the initial lead(II) concentration was over 100 mg L⁻¹. At lower concentrations, the ratio of the solute molecules to available surface sites was low, which resulted in higher biosorption rate and lower biosorption capacity. When the initial metal concentrations increased, the sites on biomass available for sorption became saturated gradually. It is necessary to identify the maximum saturation potential of a biosorbent, for which experiment should be conducted at the highest possible initial solute concentration (Vijayaraghavan and Yun 2008). As shown in Fig. 4a, higher biosorption occurred at lead(II) concentration of 125 mg L⁻¹. To balance the biosorption capacity and the removal efficiency, the suitable initial lead(II) concentration was set as 100 mg L⁻¹ under this condition, biosorption rate and biosorption capacity are 88.2% and 44.1 mg g⁻¹, respectively.

Effect of pH

To test the effect of pH on biosorption by *Alcaligenes* sp. BAPb.1, pH values were adjusted from 3 to 7, the initial lead(II) concentration was revised to 100 mg L⁻¹. It can be seen from Fig. 4b, the removal of lead(II) by BAPb.1 was strongly dependent on solution pH. Both the biosorption rate and biosorption capacity increased with pH ascending from 3 to 5, the maximum biosorption rate of 88.4% and biosorption capacity of 44.2 mg g⁻¹ were obtained at pH

Fig. 2 The physiological and biochemical characteristics of BAPb.1 (CK means control group)

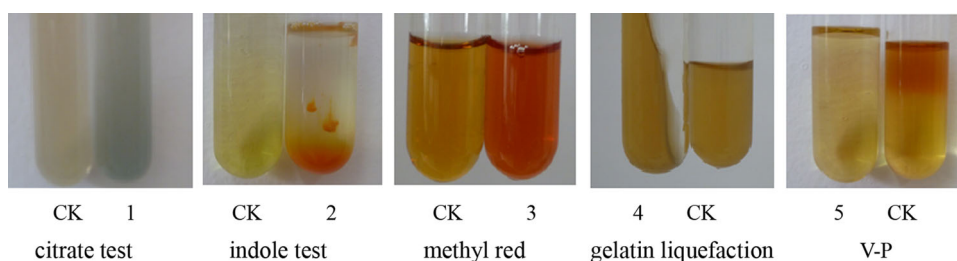
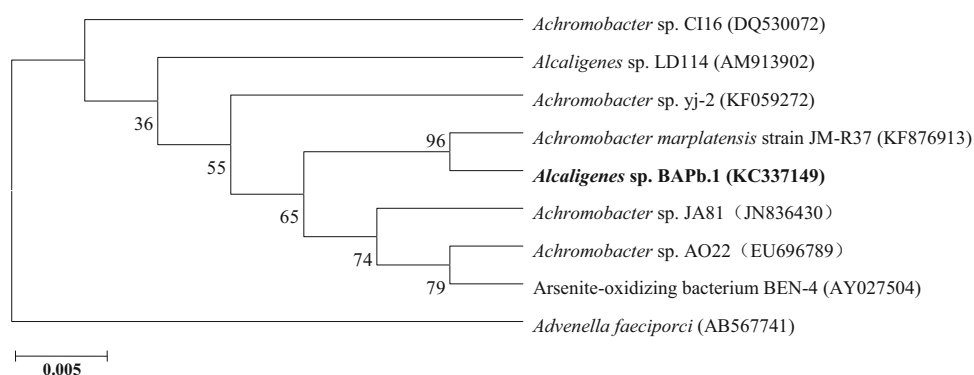


Fig. 3 Neighbor-joining tree showing the phylogenetic position of the isolate, *Alcaligenes* BAPb.1, based on the 16S rRNA gene sequence. The numbers at the nodes indicate the level of bootstrap support based on the neighbor-joining analysis of 100 replicates. Accession numbers are given in parenthesis



5. Then, both biosorption rate and biosorption capacity declined as the pH increased from 5 to 7.

At low pH (3–4), functional anionic active sites might protonate at the biosorbent surface, bringing about a large number of cationic groups in solution, which could restrict the biosorption process for lead(II) (Rodriguez et al. 2006). More carboxyl groups might dissociate from the biomass surface when the pH increased from 4 to 5.5, which enhanced ion exchange capacity of the biosorbent and improved the combination of lead ions with the anionic ligands (Hubbe et al. 2011). When the pH was higher than 7, the precipitation might occur, this process was related to insoluble metal hydroxide precipitation from the solution and should be avoided during sorption experiments to effectively distinguish between adsorption and precipitation (Onundi et al. 2010). Since the optimum pH of the biosorption process was about 5, the pH value was revised to 5 in the following experiments.

Effect of biosorbent dosage

The effect of the biosorbent dosage was investigated by varying the biosorbent amounts from 0.5 to 4.0 g L⁻¹. Figure 4c shows that the biosorption rate increased rapidly from 28 to 90% with the biosorbent dosage that increased from 0.5 to 2.0 g L⁻¹ and then kept stable when the biosorbent dosage was over 2.5 g L⁻¹. However, the biosorption capacity remained at about 58 mg g⁻¹ when the biosorbent dosage was below 1.5 g L⁻¹ and then sharply decreased with increasing biosorbent dosage. In the condition of high biosorbent dosages, the available solute was insufficient to completely cover the available exchangeable sites on the biosorbent, typically resulting in low biosorption capacity. In addition, the aggregation or overlapping of biosorbent surface area and competition for available sorption sites for metal ions adversely impacted the biosorption efficiency (EI-Sayed 2013). This result is in good agreement with those obtained in other studies (Masoudzadeh et al. 2011; Khadivinia et al. 2014). Based on the aforementioned result, the suitable biosorbent dosage was 1.5 g L⁻¹.

Effect of reaction temperature

The experimental temperature ranging from 22 to 40 °C was set to examine its effect on biosorption. Figure 4d illustrates that the biosorption rate and biosorption capacity increased from 65.6 to 86.3% and 43.7–57.5 mg g⁻¹, respectively, with the temperature rising from 22 to 30 °C. However, the results obtained in the present study showed no significant difference in biosorption rate or capacity between the lowest and highest temperatures. Energy-independent mechanisms suggest that adsorption efficiency can hardly be affected by temperature, since this biosorption is physicochemical (electrostatic forces) process in nature (Khadivinia et al. 2014). In our case, the biosorption is well performed at 30 °C, which is taken as a cost-effective temperature for practice.

Effect of contact time

The effect of contact time (from 5 to 50 min) on the removal of lead ions by BAPb.1 is shown in Fig. 4e. The process was very fast in the initial 20 min, thereafter the process became slow and reached the equilibrium at 30 min. The biosorption capacity and removal rate reached 59.2 mg g⁻¹ and 88.8% in equilibrium period, and then the amount of biosorbed lead ions did not significantly change with time. Generally, the fast process initially involved physical biosorption or ion exchange with the biomass surface and the slow biosorption process at the later stage involved micro-precipitation or complexation, primarily in the microporous structure (Ding et al. 2014; Lan et al. 2014). In this case, the amount of lead ion biosorption did not exhibit time-dependent pattern after 30 min. Therefore, the most suitable contact time was 30 min.

Biosorption isotherms

Langmuir and Freundlich isotherm models have been widely used for modeling adsorption data. Langmuir isotherm represents chemisorption and assumes a monolayer

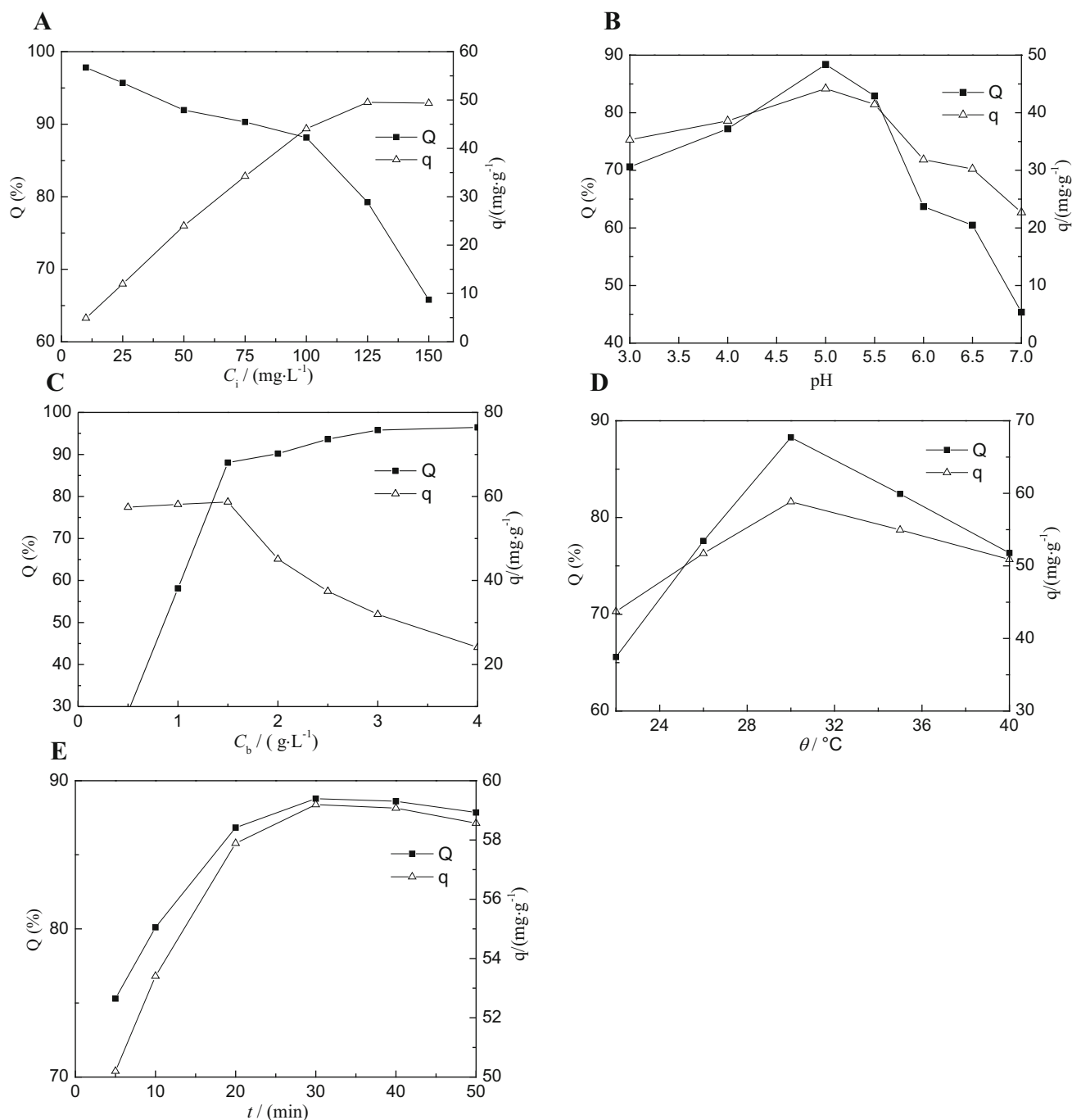


Fig. 4 Effect of physiochemical conditions on lead(II) biosorption. **a** lead(II) concentration, **b** pH, **c** biosorbent dosage, **d** temperature, **e** biosorption time

adsorption onto a surface containing a finite number of binding sites distributed homogeneously (Langmuir 1918). The Freundlich isotherm is used for modeling a heterogeneous surface of the adsorbent, indicating physisorption occurred on the adsorbent surface (Freundlich 1906). The adsorption pattern of lead(II) onto *Alcaligenes* sp. BAPb.1 was well fitted with the Langmuir and Freundlich models (Fig. 5; Table 1) whose R^2 values were 0.992 and 0.987,

respectively. Langmuir adsorption maximum, q_{\max} , was quite high with the value of 66.67 mg g⁻¹. The Langmuir equilibrium coefficient, K , was 0.0446 L mg⁻¹. Freundlich adsorption capacity, the value of k_f was 3.1076 L g⁻¹. Moreover, the Freundlich coefficient (n) was 1.283 and R^2 was 0.987. The R^2 and q_{\max} values suggested that the Langmuir isotherm might be more suitable model for the data in this study because of the high coefficients of

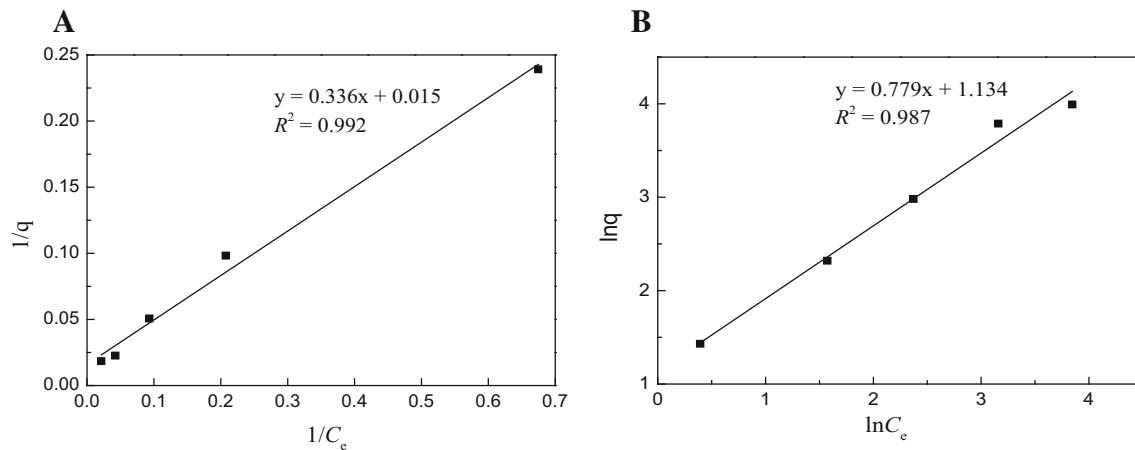


Fig. 5 Isotherms of lead(II) biosorption by BAPb.1. **a** Langmuir; **b** Freundlich

Table 1 Biosorption equilibrium constant obtained from Langmuir and Freundlich isotherms for biosorption of lead(II)

Langmuir			Freundlich		
$Q_{\max}/\text{mg g}^{-1}$	K	R^2	K_f	N	R^2
66.67	0.0446	0.992	3.1076	1.283	0.987

Table 2 Uptake capacity of lead(II) by different biosorbents

Biosorbent	$Q_{\max}/\text{mg g}^{-1}$	References
<i>Geobacillus thermodenitrificans</i>	1.29	Chatterjee et al. (2010)
<i>Staphylococcus saprophyticus</i>	100	Ilhan et al. (2004)
<i>Pseudomonas aeruginosa</i> PU21	110	Sen et al. (2014)
Hot spring consortium of microbes	74.4	Sen et al. (2014)
<i>Bacillus cereus</i>	36.7	Pan et al. (2007)
<i>Alcaligenes</i> sp. BAPb.1	66.7	This study

determination, it was concluded that monolayer biosorption occurred at specifically homogeneous sites on the cell surface of *Alcaligenes* sp. BAPb.1 (Chergui et al. 2009).

The lead biosorption capacity of *Alcaligenes* sp. BAPb.1 and other bacteria reported was shown in Table 2, it suggested that the adsorption capacity 66.7 mg g^{-1} of BAPb.1 is consistent with other bacteria; however, the different surface structure, functional groups and specific surface area of different strains result in the difference in adsorption capacity.

Biosorption mechanism

AFM analysis

Atomic force microscope has widely been used in microbiological studies to obtain topographical images of

individual bacterial cell. To evaluate the changes of surface roughness, depth and width before and after lead(II) adsorption, the two-dimensional and its corresponding three-dimensional topographic AFM images of strain BAPb.1 cells were probed and showed together with the sectional analysis in Fig. 6.

The effect of lead ions on cell ultrastructure and surface morphology can be seen in Fig. 6. Before lead(II) adsorption, the cell surface was relatively intact, smooth, homogeneous, and the sectional depth of three random points was 76.6–77.3 nm (Fig. 6a), while after lead(II) adsorption, the cell had a different pattern, some obviously collapse atrophy occurred in some areas of the cell, which led to a high degree of heterogeneity, the sectional depth of three random points was 134.9–179.1 nm (Fig. 6b); the bonding of lead(II) with polysaccharide, protein and amide existed in exopolysaccharide (EPS) contributed to the increased thickness of the cell surface (Zhang et al. 2007). The results proved that lead(II) adsorption by strain BAPb.1 involved surface adsorption and micro-precipitation. The irregular shape and topography of cell was mainly caused by the interactions between lead(II) and surface of biosorbent. Moreover, the morphological changes after lead(II) adsorption were partly attributed to the different interaction forces between the cell and substrate surfaces (Chen et al. 2014).

SEM–EDX analysis

Scanning electron microscope was used to illustrate the surface morphology of BAPb.1 before and after lead(II)

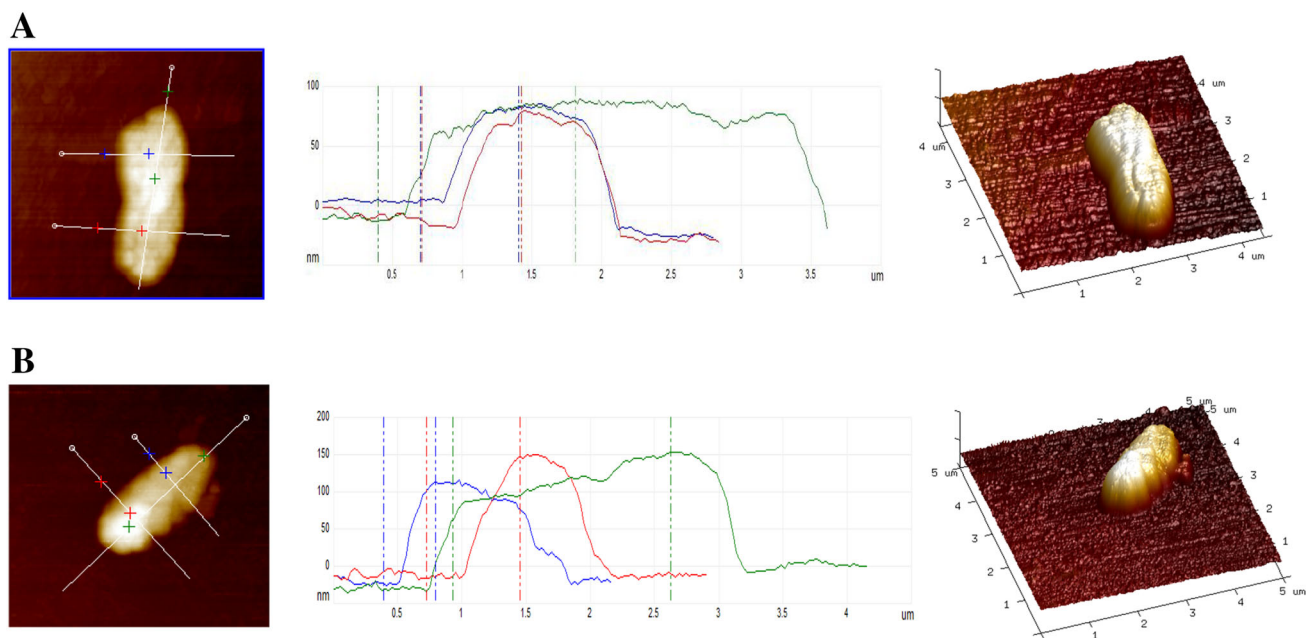
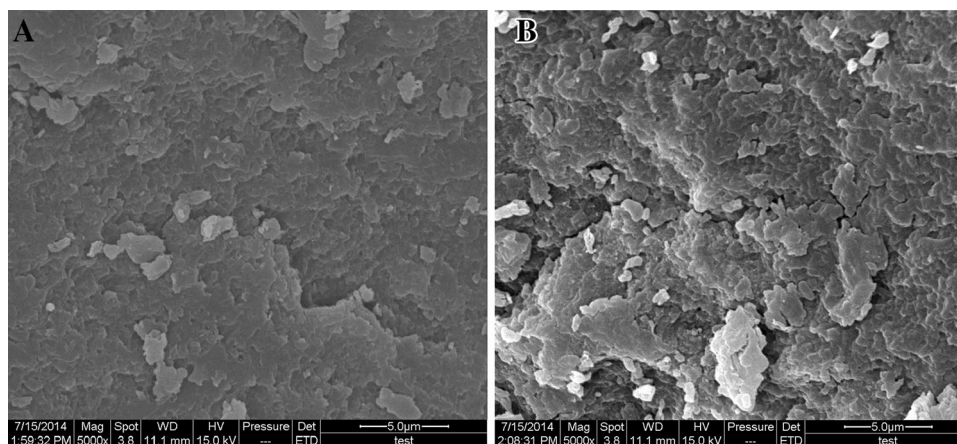


Fig. 6 AFM images of BAPb.1 before (a) and after (b) adsorbing lead(II)

Fig. 7 SEM images of BAPb.1 before (a) and after (b) adsorbing lead(II)



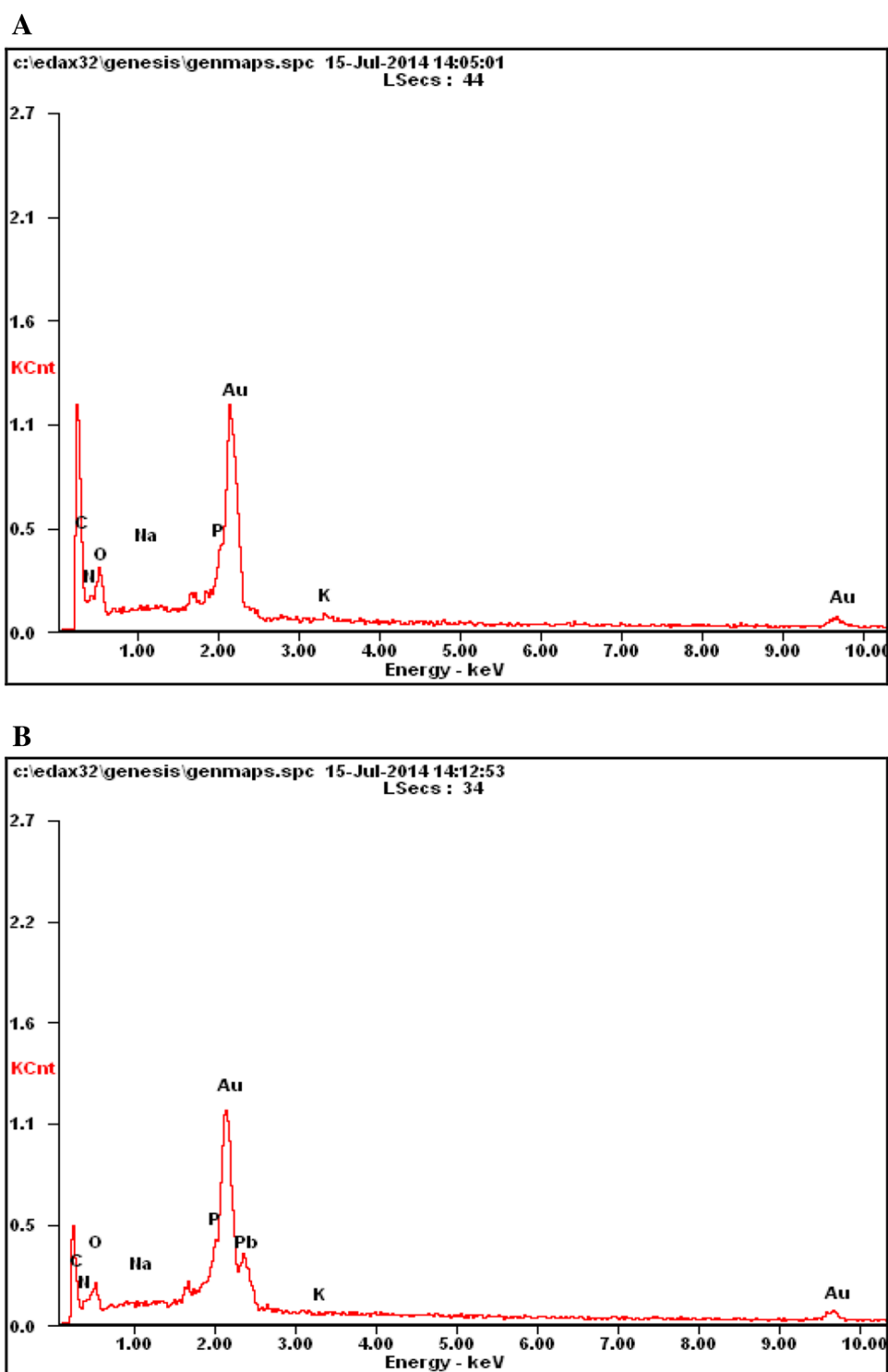
biosorption. Figure 7a shows that the original cells remained intact, smooth, and closely connected with each other, providing a large surface area for biosorption. However, after contact with lead(II), the cells appeared to shrink and wrinkle, with the bright sections displayed due to the accumulation of lead (Fig. 7b). The EDX analysis showed that the elemental composition of strain BAPb.1 significantly changed after lead(II) adsorption (Fig. 8; Table 3). The atomic percentage of element Pb (at%) was 1.77, that of C, N and O (at%) decreased, respectively, from 62.00 to 61.57, 20.7 to 19.13 and 14.19 to 13.17, while that of P increased from 2.57 to 4.11 after lead(II) uptake. The results showed that lead(II) adsorption could covalently bond with C-, N-, O- and P-containing functional groups. As previously reported, the functional groups (carboxylate, hydroxyl, amino and phosphate) on bacterial cell surface were responsible for lead(II)

adsorption (Monteiro et al. 2011; Sedighi et al. 2012). Thus, it was rational to speculate that adsorption of lead(II) by strain BAPb.1 mostly occurred on the cell surface. Moreover, atomic percentage of Na and K decreased, respectively, from 0.25 to 0.13 and 0.30 to 0.12 after contact with Pb, which revealed that Pb possibly exchanged with Na and K on the cell surface (Chojnacka et al. 2005; Kazy et al. 2006).

FTIR analysis

It is essential to identify the functional groups on the biomass involved in adsorbing process with FTIR, which is helpful to understand the surface-bonding mechanism. FTIR spectrum in and without the presence of lead(II) revealed significant differences in the absorption peaks of functional groups (Fig. 9a, b). FTIR spectrum revealed the peaks of hydroxyl

Fig. 8 EDX spectrum of BAPb.1 before (a) and after (b) adsorbing lead(II)

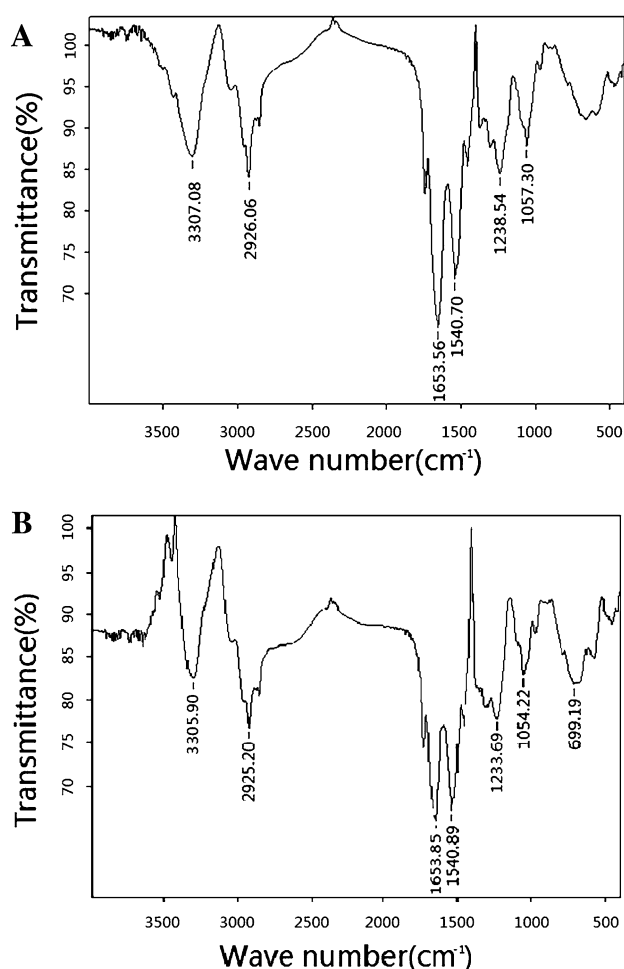


groups shifting from 3307.08 to 3305.09 cm^{-1} , at the same time the peak intensity increased and the peak width sharpened, indicating the formation of more $-\text{OH}$ complexation; anti-symmetric stretching peak of $-\text{CH}_2$ shifted from 2926.06 to 2925.20 cm^{-1} by interaction with lead(II); symmetric stretching peak of $\text{C}=\text{O}$ migrated from 1653.56 to

1653.85 cm^{-1} with the peak intensity decrease; amide $\text{C}-\text{N}$ peak shifted from 1238.54 to 1233.69 cm^{-1} and tended to be weakend; organic phosphate anti-symmetric stretching peak of $\text{P}-\text{O}-\text{C}$ shifted from 1057.30 to 1054.22 cm^{-1} ; $\text{C}-\text{S}$ peak around 699 cm^{-1} now tended to be enhanced; $\text{NH}-$ stretching around 1540 cm^{-1} was found to be responsible for lead(II)

Table 3 Elemental content analysis of BAPb.1 before and after adsorbing lead(II)

Element	Before		Element	After	
	wt%	at%		wt%	at%
CK	54.81	62.00	CK	42.99	61.57
NK	21.34	20.70	NK	15.58	19.13
OK	16.71	14.19	OK	12.25	13.17
NaK	00.42	00.25	NaK	00.17	00.13
PK	05.85	02.57	PK	07.40	04.11
PbM	–	–	PbM	21.35	01.77
KK	00.86	00.30	KK	00.27	00.12
Matrix	Correction	ZAF	Matrix	Correction	ZAF

**Fig. 9** FTIR spectra of BAPb.1 before (a) and after (b) adsorbing lead(II)

and copper(II) bonding, while the C–O bond played an important role in lead(II) sorption (Pavasant et al. 2006). Moreover, some reports stated that the presence of amino, carboxyl, hydroxyl and carbonyl groups on the surface of the

green algae *Spirogyra*, *Pseudomonas aeruginosa* ASU 6, *Enterobacter cloacae* strain P, which could be accountable for the bonding of lead (Tunali et al. 2006; Gupta and Rastogi 2008; Naik et al. 2012). These phenomena highlighted the fact that the hydroxyl, amino, amide, carbonyl, and phosphate groups were the available functional groups on *Alcaligenes* sp. BAPb.1 cell surface associated with lead(II) biosorption.

Conclusions

The strain BAPb.1 showed high resistance to lead(II), copper(II), zinc(II), nickel(II), chromium(VI), kanamycin, ampicillin, streptomycin, chloramphenicol, and tetracycline. Under the optimum biosorption conditions, the maximum biosorption rate and capacity were 85.2% and 56.8 mg g⁻¹. Equilibrium adsorption of the lead(II) by BAPb.1 biomass was well described by the Langmuir isotherm model. The biosorption mechanism includes ionic exchange interactions and complexation stages. This study reveals that the strain BAPb.1 can serve as a potential biotechnological agent to bioremediate lead contaminated waters.

Acknowledgements This research was financially supported by the Natural Science Foundation of Heilongjiang Province, China (Grant Nos. D201402 and D2016001).

Compliance with ethical standards

Conflict of interest The authors declare that they have no conflict of interest in the publication.

References

Akinbowale OL, Peng H, Grant P, Barton MD (2007) Antibiotic and heavy metal resistance in motile aeromonads and pseudomonads

- from rainbow trout (*Oncorhynchus mykiss*) farms in Australia. *Int J Antimicrob Agents* 30:177–182
- Batta N, Subudhi S, Lal B, Devi A (2013) Isolation of a lead tolerant novel bacterial species, *Achromobacter* sp. TL-3: assessment of bioflocculant activity. *Indian J Exp Biol* 51:1004–1011
- Chatterjee SK, Bhattacharjee I, Chandra G (2010) Biosorption of heavy metals from industrial waste water by *Geobacillus thermodenitrificans*. *J Hazard Mater* 175:117–125
- Chen C, Wen DH, Wang JL (2014) Cellular surface characteristics of *Saccharomyces cerevisiae* before and after Ag(I) biosorption. *Bioresour Technol* 156:380–383
- Chergui A, Kerbachi R, Junter GA (2009) Biosorption of hexacyanoferrate(III) complex anion to dead biomass of the basidiomycete *Pleurotus mutilus*: biosorbent characterization and batch experiments. *Chem Eng J* 147:150–160
- Chojnacka K, Chojnacki A, Górecka H (2005) Biosorption of Cr^{3+} , Cd^{2+} and Cu^{2+} ions by blue-green algae *Spirulina* sp.: kinetics, equilibrium and the mechanism of the process. *Chemosphere* 59:75–84
- Congeevaram S, Dhanarani S, Park J, Dexilin M, Thamaraiselvi K (2007) Biosorption of chromium and nickel by heavy metal resistant fungal and bacterial isolates. *J Hazard Mater* 146:270–277
- Ding CC, Feng S, Cheng WC, Zhang J, Li XL, Liao JL, Yang YY, An Z, Luo SZ, Yang JJ, Tang J, Liu N (2014) Biosorption behavior and mechanism of thorium on *Streptomyces sporoverrucosus* dwc-3. *J Radioanal Nucl Chem* 301:237–245
- Dong XZ, Cai MY (2001) Manual of systematic and determinative bacteriology. Science Press, Peking
- El-Sayed MT (2013) Removal of lead(II) by *Saccharomyces cerevisiae* AUMC 3875. *Ann Microbiol* 63:1459–1470
- Freundlich HMF (1906) Über die adsorption in Lösungen. *Zeitschrift für Physikalische Chemie (Leipzig)* 57:385–470
- Gabr RM, Hassan SHA, Shoreitb MAA (2008) Biosorption of lead and nickel by living and non-living cells of *Pseudomonas aeruginosa* ASU 6a. *Int Biodeterior Biodegrad* 62:195–203
- Gupta VK, Nayak A (2012) Cadmium removal and recovery from aqueous solutions by novel adsorbents prepared from orange peel and Fe_2O_3 nanoparticles. *Chem Eng J* 180:81–90
- Gupta VK, Rastogi A (2008) Biosorption of lead from aqueous solutions by green algae *Spirogyra* species: kinetic and equilibrium studies. *J Hazard Mater* 152:407–414
- Gupta VK, Srivastava SK, Mohan D, Sharma S (1998) Design parameters for fixed bed reactors of activated carbon developed from fertilizer waste for the removal of some heavy metal ions. *Waste Manage* 17:517–522
- Gupta VK, Agarwal S, Saleh TA (2011) Synthesis and characterization of alumina-coated carbon nanotubes and their application for lead removal. *J Hazard Mater* 185:17–23
- He JS, Chen JP (2014) A comprehensive review on biosorption of heavy metals by algal biomass: materials, performances, chemistry, and modeling simulation tools. *Bioresour Technol* 160:67–78
- Huang F, Dang Z, Guo CL (2013) Biosorption of Cd(II) by live and dead cells of *Bacillus cereus* RC-1 isolated from cadmium-contaminated soil. *Colloid Surf B* 107:1–18
- Hubbe MA, Hasan SH, Ducoste JJ (2011) Cellulosic substrates for removal of pollutants from aqueous systems: a review. 1. Metals. *Bioresources* 6:2161–2287
- Ilhan S, Nourbakhsh MN, Kilicarslan S, Ozdag H (2004) Removal of chromium, lead and copper ions from industrial waste waters by *Staphylococcus saprophyticus*. *Electron J Biotechnol* 2:50–57
- Kazy SK, Das SK, Sar P (2006) Lanthanum biosorption by a *Pseudomonas* sp.: equilibrium studies and chemical characterization. *J Ind Microbiol Biotechnol* 33:773–783
- Khadivinia E, Sharafi H, Hadi F, Zahiri HS, Modiri S, Tohidi A, Mousavi A, Salmanian AH, Noghahi KA (2014) Cadmium biosorption by a glyphosate-degrading bacterium, a novel biosorbent isolated from pesticide-contaminated agricultural soils. *J Ind Eng Chem* 20:4304–4310
- Khani H, Rofouei MK, Arab P, Gupta VK, Vafaei Z (2010) Multi-walled carbon nanotubes-ionic liquid-carbon paste electrode as a super selectivity sensor: application to potentiometric monitoring of mercury ion(II). *J Hazard Mater* 183:402–409
- Lan T, Feng Y, Liao JL, Li XL, Ding CC, Zhang D, Yang JJ, Zeng JH, Yang YY, Tang J, Liu N (2014) Biosorption behavior and mechanism of cesium-137 on *Rhodospiridium fluviale* strain UA2 isolated from cesium solution. *J Environ Radioactiv* 134:6–13
- Langmuir I (1918) The adsorption of gases on plane surfaces of glass, mica and platinum. *J Am Chem Soc* 40:1361–1403
- Latha S, Vinothini G, Dhanasekaran D (2015) Chromium [Cr(VI)] biosorption property of the newly isolated actinobacterial probiont *Streptomyces werraensis* LD22. *3 Biotech* 5:423–432
- Liu YJ, Pei X, Lin H, Gai P, Liu YC, Wu ZL (2012) Asymmetric bioreduction of activated alkenes by a novel isolate of *Achromobacter* species producing enoate reductase. *Appl Microbiol Biotechnol* 95:635–645
- Masoudzadeh N, Zakeri F, Lotfabad TB, Sharafi H, Masoomi F, Zahiri SH, Ahmadian G, Noghahi KA (2011) Biosorption of cadmium by *Brevundimonas* sp. ZF12 strain, a novel biosorbent isolated from hot-spring waters in high background radiation areas. *J Hazard Mater* 197:190–198
- Monteiro CM, Castro PML, Malcata FX (2011) Biosorption of zinc ions from aqueous solution by the microalga *Scenedesmus obliquus*. *Environ Chem Lett* 9:169–176
- Naik MM, Pandey A, Dubey SK (2012) Biological characterization of lead-enhanced exopolysaccharide produced by a lead resistant *Enterobacter cloacae* strain P2B. *Biodegradation* 23:775–783
- Ng SP, Davis B, Palombo EA, Bhave M (2009) A Tn5051-like mer-containing transposon identified in a heavy metal tolerant strain *Achromobacter* sp. AO22. *BMC Res Notes* 2:42–49
- Onundi YB, Mamun AA, Khatib MFA, Ahmed YM (2010) Adsorption of copper, nickel and lead ions from synthetic semiconductor industrial wastewater by palm shell activated carbon. *J Environ Sci Tech* 7:751–758
- Özcan AS, Tunali S, Akar T, Özcan A (2009) Biosorption of lead(II) ions onto waste biomass of *Phaseolus vulgaris* L.: estimation of the equilibrium, kinetic and thermodynamic parameters. *Desalination* 244:188–198
- Pan JH, Liu RX, Tang HX (2007) Surface reaction of *Bacillus cereus* biomass and its biosorption for lead and copper ions. *J Environ Sci China* 19:403–408
- Pavasant P, Apiratikul R, Sungkhum V, Suthiparinyanont P, Wattanachira S, Marhaba TF (2006) Biosorption of Cu^{2+} , Cd^{2+} , Pb^{2+} , and Zn^{2+} using dried marine green macroalga *Caulerpa lentillifera*. *Bioresour Technol* 97:2321–2329
- Puyen ZM, Villagrana E, Maldonado J, Diestra E, Esteve I, Solé A (2012) Biosorption of lead and copper by heavy-metal tolerant *Micrococcus luteus* DE2008. *Bioresour Technol* 126:233–237
- Ren GM, Jin Y, Zhang CM, Gu HD, Qu JJ (2015) Characteristics of *Bacillus* sp. PZ-1 and its biosorption to Pb(II). *Ecotoxicol Environ Saf* 117:141–148
- Rodriguez CE, Quesada A, Rodriguez E (2006) Nickel biosorption by *Acinetobacter baumannii* and *Pseudomonas aeruginosa* isolated from industrial wastewater. *Braz J Microbiol* 37:465–467
- Saleh TA, Gupta VK, Al-Saadi AA (2013) Adsorption of lead ions from aqueous solution using porous carbon derived from rubber tires: experimental and computational study. *J Colloid Interface Sci* 396:264–269

- Sedighi M, Ghasemi M, Hassan SHA, Wan RWD, Ismail M, Abdallah E (2012) Process optimization of batch biosorption of lead using *Lactobacillus bulgaricus* in an aqueous phase system using response surface methodology. *World J Microbiol Biotechnol* 28:2047–2055
- Sen SK, Raut S, Dora TK, Mohapatra PKD (2014) Contribution of hot spring bacterial consortium in cadmium and lead bioremediation through quadratic programming model. *J Hazard Mater* 265:47–60
- Sheng XF, Xia JJ, Jiang CY, He LY, Qian M (2008) Characterization of heavy metal-resistant endophytic bacteria from rape (*Brassica napus*) roots and their potential in promoting the growth and lead accumulation of rape. *Environ Pollut* 156:1164–1170
- Souza MJD, Nair S, Bharathi PAL, Chandramohan D (2006) Metal and antibiotic-resistance in psychrotrophic bacteria from Antarctic marine waters. *Ecotoxicology* 15:379–384
- Tripathi M, Vikram S, Jain RK, Garg SK (2011) Isolation and growth characteristics of chromium(VI) and pentachlorophenol tolerant bacterial isolate from treated tannery effluent for its possible use in simultaneous bioremediation. *Indian J Microbiol* 51:61–69
- Tunali S, Çabuk A, Akar T (2006) Removal of lead and copper ions from aqueous solutions by bacterial strain isolated from soil. *Chem Eng J* 115:203–211
- Ucuna H, Aksakal O, Yildiz E (2009) Copper(II) and zinc(II) biosorption on *Pinus sylvestris* L. *J Hazard Mater* 161:1040–1045
- Vijayaraghavan K, Yun YS (2008) Bacterial biosorbents and biosorption. *Biotechnol Adv* 26:266–291
- Zhang DY, Wang JL, Pan XL (2007) Cadmium sorption by EPSs produced by anaerobic sludge under sulfate-reducing conditions. *J Hazard Mater* 138:589–593
- Zhu CW, Li ZP, Li DC, Xin Y (2014) Pb tolerance and bioaccumulation by the mycelia of *Flammulina velutipes* in artificial enrichment medium. *J Microbiol* 52:8–12